The nature of the vortical structures in the near wake of the Ahmed body.

Journal Title
XX(X):1–6

DOI: 10.1177/ToBeAssigned
www.sagepub.com/
SAGE

J. Venning[1], D. Lo Jacono[2], D. Burton[3], M. C. Thompson[1], and J. Sheridan[1]

Abstract

This study presents the results from high-spatial-resolution water-channel velocity-field measurements behind an *Ahmed body* with 25° rear slant angle. The Ahmed body represents a simplified generic model of a hatchback automobile that has been widely used to study near-wake flow dynamics. The results help clarify the unresolved question of whether the time-mean near-wake flow structure is topologically equivalent to a toroidal vortex or better described by a pair of horizontally aligned horseshoe vortices, with their legs pointing downstream. The velocimetry data presented allows the tracking of the vortical structures throughout the near wake through a set of orthogonal planes, as well as the measurement of their circulation. The spanwise vortices that form as the flow separates from the top and bottom rear edges are shown to tilt downstream at the sides of the body, while no evidence is found of a time-mean attached toroidal vortex, at least for the Reynolds number (based on the square root of frontal area) of $Re_{\sqrt{FA}} \sim 30,000$ under consideration.

Keywords

Ahmed body, PIV, vortices.

Introduction

The Ahmed body[1] is a widely accepted standardised body used to investigate vehicle aerodynamics. It has been previously studied in great depth, with particular focus on the effects of the rear slant angle on the wake structures and drag force. In the high drag case (25°, Figure 1), the time-averaged wake consists of three main three-dimensional structures:

(a) The A vortical structure that is formed by the recirculation as the flow separates at the top of the vertical back surface of the model.

(b) The B vortical structure that is formed due to the separation on the base of the model.

(c) The C-pillar vortices that form as the vorticity in the side boundary layers roll up over the slant edges.

This paper focusses on the A and B vortices, the natures of which are widely debated in the literature. Some studies[2–8] refer to these regions as a torus, similar to the toroidal wake of a cube or square-backed Ahmed model[9;10], although it is now recognised that this torus may only be present when considering a long time-average[11] or a summation of two modes[12]. Other interpret these structures behind the high drag body as two horseshoe vortices[1;13;14]. It has even been suggested[15] both that the vortex cores form a "ring-like vortex" and that they are two horseshoe vortices with A tilting downstream and B tilting vertically. While ample evidence is presented[10] to show that a torus is present behind the *time-averaged* square-back body, there is a limited understanding on how these structures are organized in the high-drag (25°) case.

A PIV survey of the Ahmed wake[14] presented data showing an increase in streamwise circulation in the C-pillar vortex further downstream than the back of the body. Since vorticity, and hence circulation, cannot be produced anywhere except on the surface of the body, it was proposed that the A vortex feeds into the C-pillar vortex, causing the increase.

This paper seeks to provide a better understanding to the nature of the flow physics in these regions by supplying time-averaged PIV data behind the base of the model that is highly resolved spatially. The intention is to resolve the present question on whether these structures are toroidal or not.

Experimental setup

The model used in this experiment was a one-quarter scale of Ahmed's original geometry with rear slant angle of 25°. It was manufactured out of Acetal and mounted to a ground-plane with two symmetric airfoils. The ground plane extended $4.2H$ (body heights) upstream

[1]Fluids Laboratory for Aeronautical and Industrial Research (FLAIR) Department of Mechanical and Aerospace Engineering, Monash University, Clayton, VIC 3800, Australia
[2]Institut de Mécanique des Fluides de Toulouse (IMFT), CNRS, UPS, Université de Toulouse, Allée Camille Soula, F-31400 Toulouse, France
[3]Department of Mechanical and Aerospace Engineering, Monash University, Victoria, Australia.

Corresponding author:
James Venning, Department of Mechanical and Aerospace Engineering, Monash University, Victoria, Australia.
Email: james.venning@gmail.com

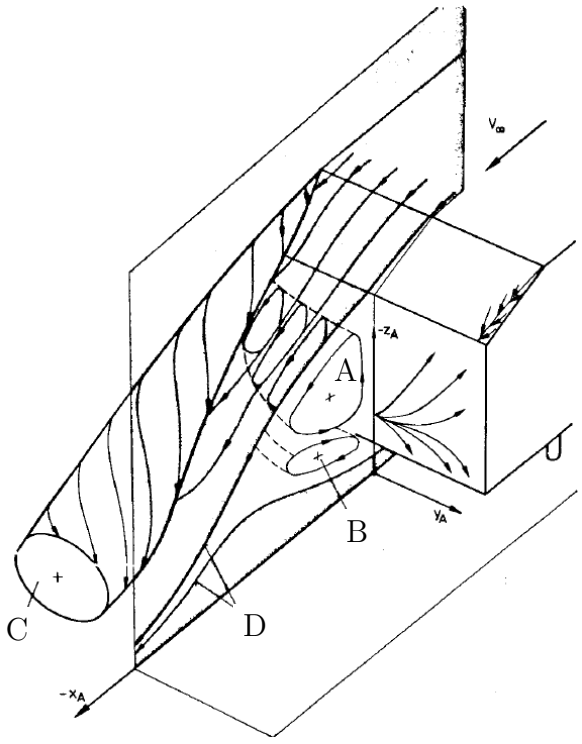

Figure 1. Structures in the wake of the Ahmed body[1]. The labels A and B are used throughout the text to refer to the vortices so labelled in this schematic.

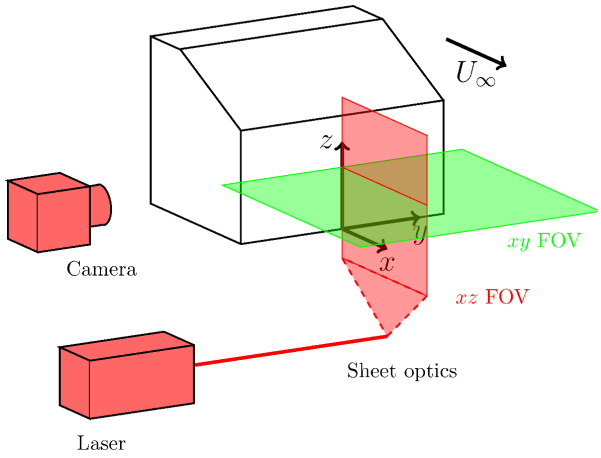

Figure 2. Schematic of the experimental setup. The camera and laser positions are correct only for the xz acquisition planes (FOV), as shown in red. For the xy planes (in green), the camera is placed below the channel and the laser is positioned where the camera is in this schematic. The origin of the coordinate planes is at the base of the rear surface of the model, in the symmetry plane. Only a single xz and xy plane are included for clarity.

Table 1. PIV Parameters for the two different measurement planes.

	xz	xy
No. of pairs	1500	1500
Δt	2 ms	2 ms
Framerate	10 Hz	10 Hz
Magnification	29.5 px/mm	17.7 px/mm
Field of View	$0.26L \times 0.94H$	$0.44L \times 1.17W$
Vectors	249×249	249×249

of the leading edge of the model and had a 4:1 elliptical leading edge. The boundary layer was measured to be one-third of the ground clearance, and the displacement thickness one-tenth. This setup was validated[14] and shown to produce the major flow structures expected of the Ahmed wake.

The model was tested in the FLAIR (Fluids Laboratory for Aeronautical and Industrial Research) water channel at Monash University, Victoria. The water channel is a free-surface, closed circuit channel with cross-section 600 mm wide × 800 mm high and is 4000 mm long. With a freestream velocity of 0.365 ms^{-1}, the Reynolds number based on the square-root of the standard body frontal area (FA) was $\mathrm{Re}_{\sqrt{FA}} = 3 \times 10^4$. The inflow conditions had turbulence levels (I_u) of less than 0.5% and non-uniformity of ± 1% across the usable test section.

The flow was seeded with Vestosint spherical particles (Vestosint, Germany) with density 1.016 $\mathrm{g/cm}^3$ and mean size 56 µm. A 5 W continuous laser (CNI, China) was used to illuminate these particles behind the vertical back of the Ahmed model. The laser emitted light with wavelength 532 nm, passing through a planar-convex lens to spread the beam into a 2 mm thick laser sheet. Seventeen equi-spaced vertical (xz) planes from $y/W = -0.103$ to $y/W = 0.720$ ($\Delta y = 5$ mm) and twelve equi-spaced spanwise (xy) planes from $z/H = 0$ to $z/H = 1.108$ ($\Delta z = 5$ mm) that were acquired using a PCO Dimax S4 (PCO, Germany) camera (resolution 2016×2016) with a Nikkor 105 mm lens. Since a continuous wave laser was used for illumination, the exposure control of the camera was used to control the light level of each recorded image. Figure 2 shows the location of the PIV planes relative to the body. The PIV parameters used at each acquisition plane are given in Table 1. The image pairs were analyzed using in-house cross-correlation software with a window size of 32 × 32 pixels and an overlap of 75% to estimate the two components of velocity in the image plane. The software was originally described in[16] for the more complicated case of target-free stereo PIV, although only the iterative multi-window processing technique for a single camera is required here. It has been subsequently further developed and updated since[14;17;18].

Results

Figure 3 (a) shows the velocity field in the body's symmetry plane. The recirculation regions A and B are evident as a pair of counter-rotating vortices behind the base of the model. The Γ_1 criterion[19] is used to highlight regions of local rotation throughout the flow. As is evident in Figure 3, the maximum and minimum of Γ_1 correspond to the cores of the A and B vortical structures respectively. If a plane further towards the edge of the body is considered, Figure 3 (b-c), the regions become much less defined. Once the plane at $y/W = 0.411$ is reached, the Γ_1 criteria no longer detects the cores of these regions.

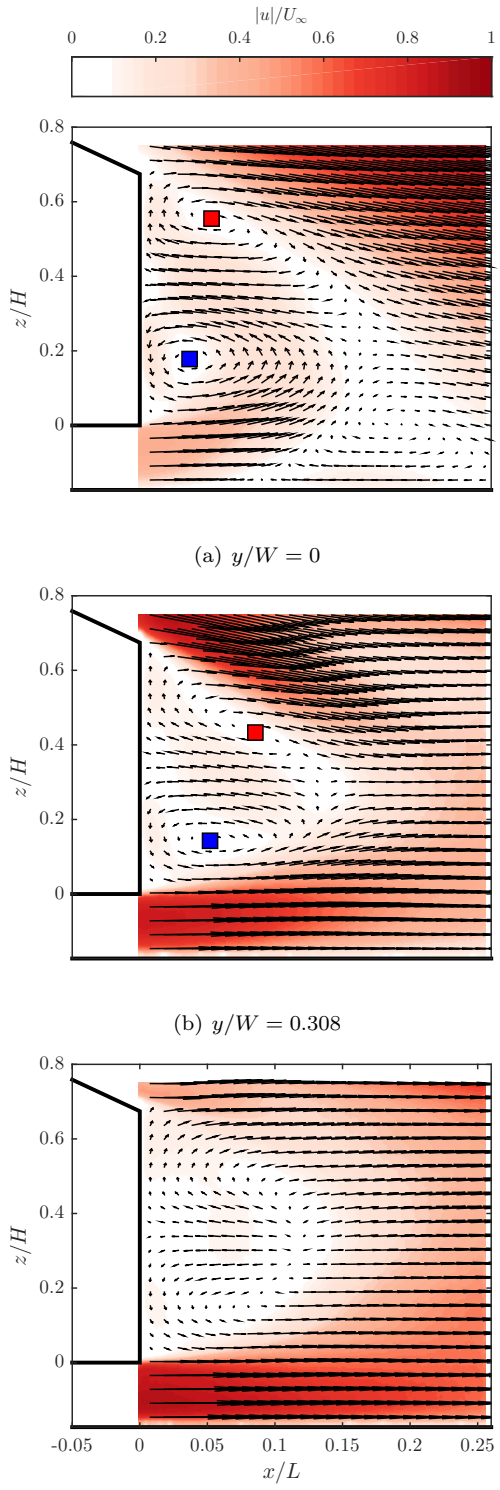

(a) $y/W = 0$

(b) $y/W = 0.308$

(c) $y/W = 0.411$

Figure 3. Flow in xz planes behind the Ahmed model with velocity vectors overlaid onto contours of total velocity magnitude. Only one in one hundred velocity vectors are shown for clarity. Red and blue points indicate the core of the A and B vortical structures respectively, found as the maximum and minimum of Γ_1 respectively.

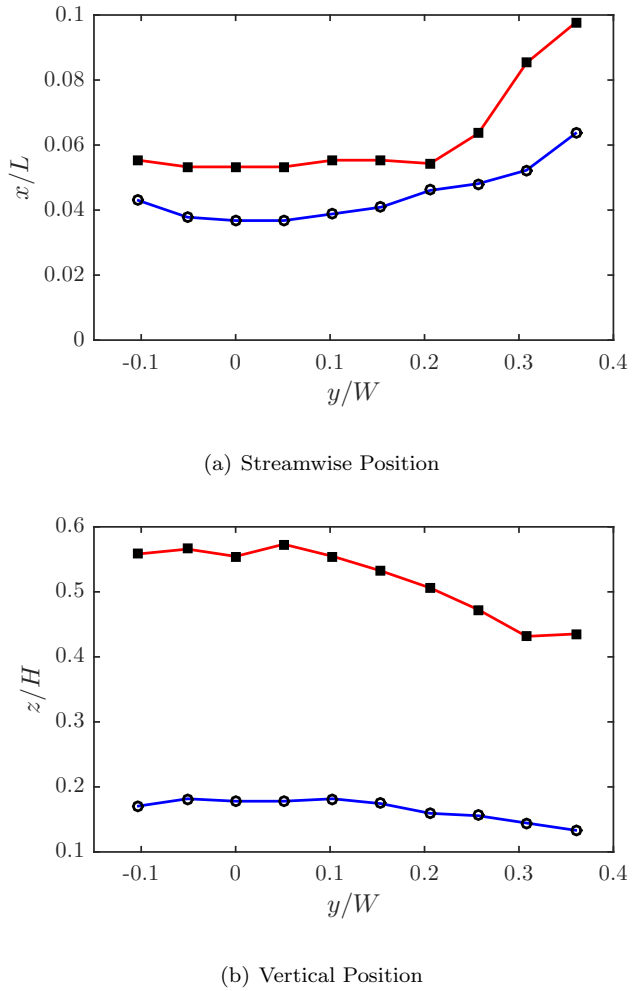

(a) Streamwise Position

(b) Vertical Position

Figure 4. Core location of the A (red, squares) and B (blue, circles) vortical structures against spanwise position.

Due to the high spatial density of the xz PIV planes the cores of the vortices can be tracked across the span (Figure 4). For $y/W < 0.2$, the streamwise location of both the A and B cores increases slightly, indicating a bend in the core. After $y/W = 0.2$, the streamwise position suddenly increases, especially of the A region, due to the bending of the region by the streamwise flow coming around the sides of the body. No data can be presented for planes beyond $y/W = 0.4$ because the region is so ill-defined that its core location cannot be determined, that is, there is no core hence no core can be located (Figure 3 (c)).

Figure 5 shows isosurfaces of spanwise Γ_1, giving the spatial evolution of the recirculation regions across the span. Close to the edge of the body, the A region tilts more into the streamwise direction than it does downwards. This is as expected if the regions were horseshoe vortices as opposed to a vortex torus or ring.

The circulation bound in each of these regions was extracted through integration of the velocity field. Figure 6 shows how the circulation varies with spanwise position. The circulation in region B linearly decreases in magnitude with spanwise position, but region A has a more abrupt decrease. As the circulation is varying, and since circulation cannot be created except at the boundary of the body, some of the circulation must be tilted into another direction. This could be either the streamwise, supporting the twin-horseshoe interpretation, or the vertical direction, suggesting the vortex takes a toroidal shape.

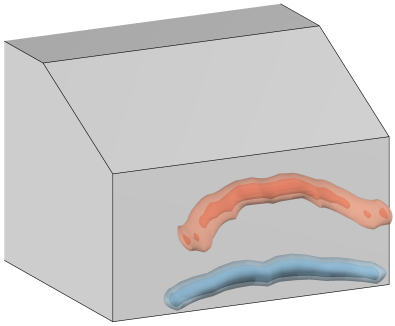

(a) Isometric view

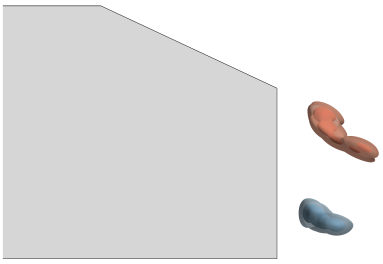

(b) Side view

Figure 5. Three-dimensional representations of spanwise Γ_1 criterion. Red represents positive rotation (A region), blue represents negative rotation (B region). Colours are consistent with Figure 4.

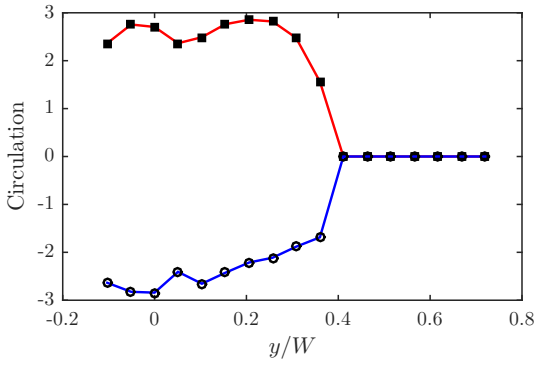

Figure 6. The spanwise circulation bound in the A (red, squares) and B (blue, circles) vortical structures against spanwise position. Circulation is non-dimensionalised with the free-stream velocity and the square-root of the frontal area.

If these structures were joined in a torus shape, one would expect to see rotating flow due to these structures in horizontal planes taken at a range of heights along the back surface. Figure 7 shows such a plane; clearly there is no rotation in the expected regions of the torus. For comparison, a PIV slice through the mid-height of a square-back Ahmed body is shown in Figure 7 (b), demonstrating the vertical vortices that are present within a toroidal wake. The contrast shown here is

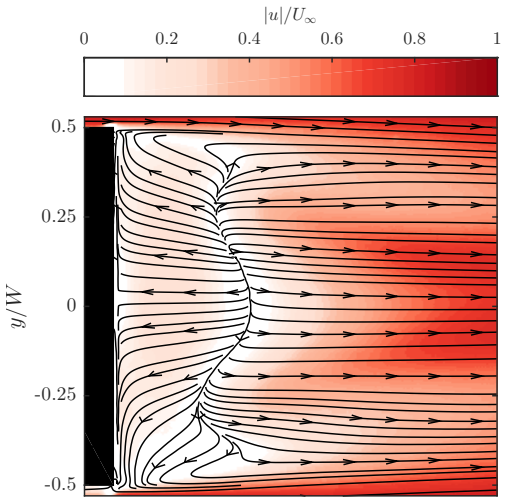

(a) 25° slant

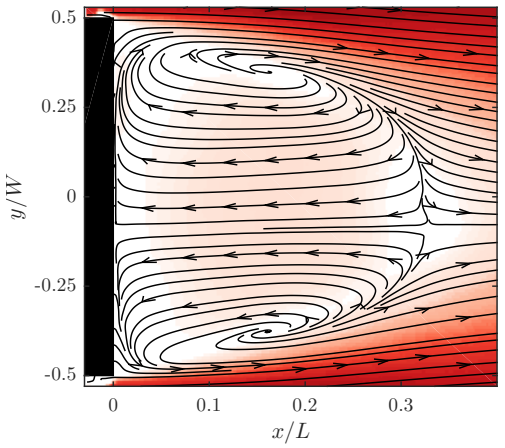

(b) Square-back

Figure 7. (a) Flow in the xy plane at $z/H = 0.369$ with velocity streamlines overlaid onto filled contours of total velocity. (b) Flow behind the square-back Ahmed geometry at the mid-height plane clearly showing the vertical legs of the toroidal vortex. Streamlines are used to indicate the local flow direction only.

quite stark, but the only difference between the two experiments is the rear slant angle changing to 0°. If the vortices were horseshoes as proposed, the trailing legs of these would be seen in a plane orthogonal to the main flow. Such an experiment was performed[20] where the laser plane for PIV was parallel to the rear surface of the body. This has been reproduced in Figure 8. Here the B vortex is seen at the base of the model. The upper vortex contains both the A and C-pillar vortices[14]. On the negative y side, the A vortex can be seen separately and below the C-pillar vortex, before they fully merge.

The velocity data from the two different orientations was reconstructed into a three-dimensional velocity field, comprising all three velocity components in a volume located behind the base. Three-dimensional streamribbons are presented in Figure 9. These were generated by seed points in and around the A and B vortical structures. Particularly for the lower (B) region, a very cohesive picture is shown of flow rolling up into

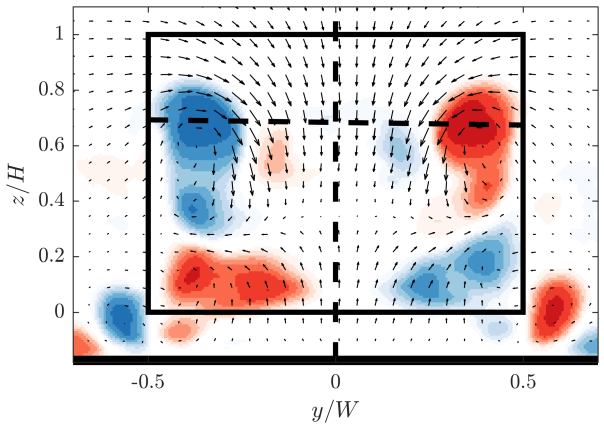

Figure 8. Cross-stream PIV plane $0.1L$ behind the high-drag Ahmed model showing the trailing legs of the B vortex as well as the combined A and C-pillar vortices. One in sixty-four vectors are displayed for clarity. Filled contours are Γ_2 ranging from -1 in blue (clockwise rotation) to 1 in red (counter-clockwise rotation). Reproduced from [20] with permission.

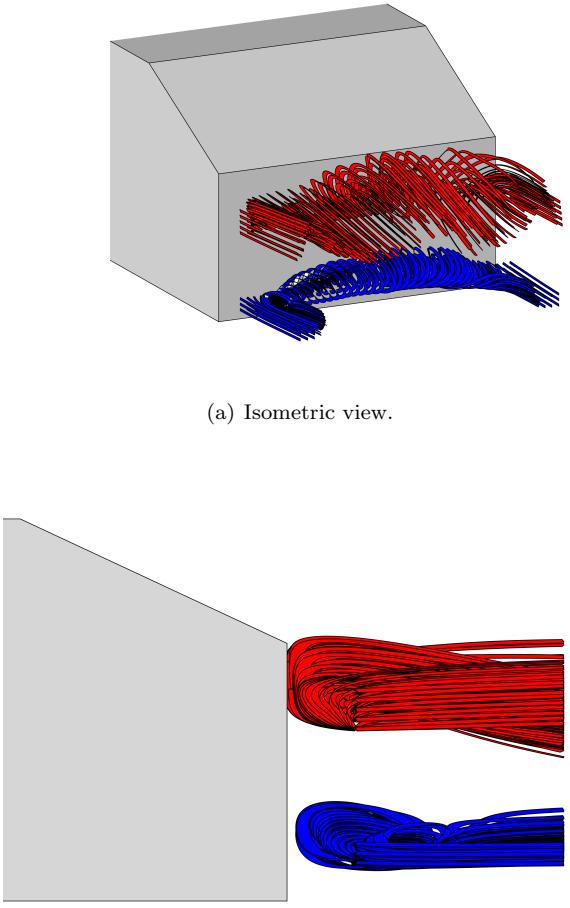

(a) Isometric view.

(b) Side view.

Figure 9. Streamribbons with seed points in the A (red) and B (blue) regions. Especially in the B region, spanwise flow is clearly evident until the edge of the body, where the streamribbons are tilted in the streamwise direction.

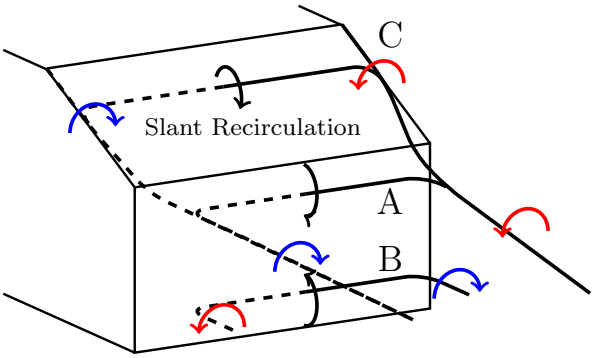

Figure 10. Vortex structure schematic in the wake of the Ahmed body, with lines indicating the location of vortex cores. The structure is dashed for $y/W < 0$ and solid for $y/W > 0$. Spanwise rotation indicated by black arrows, streamwise rotation indicated by red or blue arrows for positive or negative rotation respectively.

the core of the vortex and being transported to the sides of the body. Notice that all of the blue streamribbons, which are seeded uniformly across the span, ultimately move downstream only at the edges of the body. This demonstrates that there is sufficient spanwise flow to move all the fluid at the centre of the body that is within the B vortex to the edges of the body. As the flow reaches the edge of the body, the shear of the essentially free-stream velocity in the streamwise direction causes the streamribbons to tilt into that direction. This is further support for the theory that the A and B vortices are in fact two horseshoe shaped vortices situated above each other.

When the same procedure is followed for region A, the flow pattern is less coherent. The recirculatory nature of the flow is still evident, but the vortex is not as coherent as B, neither is the spanwise flow as strong. This is understandable as the B region is produced by a high shear region of near free-stream velocity reaching the low pressure region and rolling around the bottom edge. For the A region, the flow is first separated at the top of the slant, and reattaches (in the mean flow sense) at the end of the slant, shortly before it separates again and forms the A region.

Since the A vortex is tilted in the streamwise direction, the vortex core is now parallel with, and close to, the C-pillar vortex. It is hypothesised that these structures would merge. This hypothesis has been presented before [14] by using the sudden increase of circulation in the C-pillar vortex to suggest the merging of the A and C-pillar structures. The data in this present paper support this view. The suggested wake structure is schematised in Figure 10, where the cores of each of the regions are indicated by solid lines.

Conclusions

This paper presents a strong case that the time-mean near-wake behind the vertical surface of the Ahmed body at moderate Reynolds numbers is comprised of two horseshoe vortices, as opposed to the toroidal shape some suggest. This is shown through high spatial-

resolution velocity fields taken in orthogonal planes close to the body showing the roll-up of the vortical structures along both horizontal edges of the Ahmed base, but no such formation on the vertical edges.

The circulation along the span was quantified and shown to be decreasing near the side edges of the body. Due to Kelvin's theorem, this indicates the tilting of circulation into another plane. The three-dimensional representations of the data show that this other plane is the streamwise direction rather than the vertical direction, showing this structure to not be toroidal. This data provides further support for the hypothesis that the circulation from the A-region in fact feeds into and strengthens the C-pillar trailing vortices[14].

Acknowledgements

The authors would like to thank Mr. J. Meikle for the assistance in data acquisition for this paper.

Funding

The authors would also like to acknowledge the financial support of the Australian Research Council (ARC) through Linkage Project LP0991170 and the Centre National de la Recherche Scientifique (CNRS) through Grant No. PICS161793 under the Projet International de Cooperation Scientifique.

Declaration of conflicting interests

The authors declare that there is no conflict of interest.

References

1. Ahmed SR, Ramm G and Faitin G. Some salient features of the time-averaged ground vehicle wake. Technical report, Society of Automotive Engineers, Inc., Warrendale, PA, 1984.
2. Kourta A and Leclerc C. Characterization of synthetic jet actuation with application to Ahmed body wake. *Sensors and Actuators, A: Physical* 2013; 192: 13–26.
3. Beaudoin JF and Aider JL. Drag and lift reduction of a 3d bluff body using flaps. *Experiments in Fluids* 2008; 44(4): 491–501.
4. Beaudoin JF, Cadot O, Aider JL et al. Cavitation as a complementary tool for automotive aerodynamics. *Experiments in Fluids* 2004; 37(5): 763–768.
5. Joseph P, Amandolèse X and Aider JL. Drag reduction on the 25° slant angle Ahmed reference body using pulsed jets. *Experiments in Fluids* 2011; : 1–17.
6. Drouin V, Giovannini A and Gilliéron P. Topology and characterisation of the vortical near-wake flow over a simplified car model. In *Conference on Bluff Body Wakes and Vortex-Induced Vibrations (BBVIV3)*. pp. 1–4.
7. Wang XW, Zhou Y, Pin YF et al. Turbulent near wake of an Ahmed vehicle model. *Experiments in Fluids* 2013; 54(4).
8. Zhang BF, Zhou Y and To S. Unsteady flow structures around a high-drag Ahmed body. *Journal of Fluid Mechanics* 2015; 777: 291–326.
9. Rouméas M, Gilliéron P and Kourta A. Analysis and control of the near-wake flow over a square-back geometry. *Computers & Fluids* 2009; 38(1): 60–70.
10. Grandemange M, Gohlke M and Cadot O. Turbulent wake past a three-dimensional blunt body. part 1. Global modes and bi-stability. *Journal of Fluid Mechanics* 2013; 722: 51–84.
11. Evrard A, Cadot O, Herbert V et al. Fluid force and symmetry breaking modes of a 3d bluff body with a base cavity. *Journal of Fluids and Structures* 2016; 61: 99–114.
12. Perry AK, Pavia G and Passmore M. Influence of short rear end tapers on the wake of a simplified square-back vehicle: wake topology and rear drag. *Experiments in Fluids* 2016; 57(11): 169.
13. Franck G and El JD. Cfd modeling of the flow around the Ahmed vehicle model. In *Proceedings of 2nd conference on advanced and applications of GiD*. pp. 5–8.
14. Venning J, Lo Jacono D, Burton D et al. The effect of aspect ratio on the wake of the Ahmed body. *Experiments in Fluids* 2015; 56(6).
15. Krajnović S and Davidson L. Flow around a simplified car, part 2: Understanding the flow. *Journal of Fluids Engineering* 2005; 127(5): 919.
16. Fouras A, Lo Jacono D and Hourigan K. Target-free stereo PIV: a novel technique with inherent error estimation and improved accuracy. *Experiments in Fluids* 2007; 44(2): 317–329.
17. Sherry M, Nemes A, Lo Jacono D et al. The interaction of helical tip and root vortices in a wind turbine wake. *Physics of Fluids* 2013; 25(11): 1–16.
18. Nemes A, Lo Jacono D, Blackburn HM et al. Mutual inductance of two helical vortices. *Journal of Fluid Mechanics* 2015; 774: 298–310.
19. Graftieaux L. Combining PIV, POD and vortex identification algorithms for the study of unsteady turbulent swirling flows. *Measurement Science and Technology* 2001; 1422.
20. Venning J. *Vortex structures in the wakes of two- and three-dimensional bodies*. PhD Thesis, Monash University, 2015.